

Supporting Information for:

Hydroxamate Anchors for Water-Stable Attachment to TiO₂ Nanoparticles

William R. McNamara, Robert C. Snoeberger III, Gonghu Li, Christiaan Richter, Laura J. Allen, Rebecca L. Milot, Charles A. Schmuttenmaer,* Robert H. Crabtree,* Gary W. Brudvig,* and Victor S. Batista*
Yale University, Department of Chemistry, New Haven, Connecticut, 06520-8107.

April, 2009

This PDF file includes:

Methods and Models

- Synthesis and Characterization of **2**.
- Sample Preparation
- EPR Spectroscopy
- Surface Coverage Determination
- Time-Resolved Terahertz Spectroscopy Measurements
- Computational Procedures

Figures S1–S5.

- S1. Diffuse reflectance IR of **2** and **2-TiO₂**
- S2. UV-vis of **2-TiO₂** and N719-TiO₂
- S3. UV-vis of water stability of **2-TiO₂**
- S4. ¹H NMR spectrum of **2**
- S5. ¹³C NMR spectrum of **2**

I. Synthesis and Characterization of **2**

1 was prepared by literature methods.¹ To a mixture of **1** (0.612 mmol) and BnONH₂ (0.612 mmol) in 15 mL of THF at room temperature, 3.1 eq of 1 M LiHMDS was added (1.90 mL, 1.90 mmol) dropwise. The solution was then stirred at room temperature for 30 minutes. The resulting yellow solution was quenched with the addition of saturated NH₄Cl and extracted 3 times with ethyl acetate. The combined organic layers were dried over magnesium sulfate, filtered, and the solvent removed under vacuum. The crude product was then dissolved in dry ethanol with Pd/C (10% by weight) and stirred at room temperature. To this mixture, 1 atm of H₂(g) was added and stirred 12 hours at room temperature. The resulting solution was filtered through celite and the solvent was removed under vacuum. The resulting solid was suspended in hexanes, collected by vacuum filtration, and rinsed with additional hexanes to yield 0.289 mmol of **2** (47 % yield). ¹H NMR (CD₃OD, 400 MHz): δ 8.68–8.58 (m, 6H), 8.12–7.85 (m, 6H, CH_{AR}), 7.50 (t, 2H), 7.32–7.29 (s, 1H, NH), 4.57 (s, 1H, OH). ¹³C NMR (CD₃OD, 500 MHz): δ 158.93, 148.89, 148.55, 142.02, 141.62, 134.08, 130.27, 125.84, 120.53, 119.85, 117.03, 114.43, 111.29. Mass Spectroscopy: ES molecular ion calculated for C₂₂H₁₇N₄O₂⁺: 369.1352; found m/z: 369.1346.

II. Sample Preparation

*1. Sensitization of TiO₂ with **2***

Sensitized TiO₂ nanoparticles were prepared by stirring 30 mg of Degussa P25 TiO₂ nanoparticles (NPs) in 4 mL of a 0.9 mM solution

of **2** in dry ethanol at room temperature for 12 hours. The resulting suspension was centrifuged to pellet the sensitized nanoparticles. The supernatant was then decanted, and the remaining pelleted particles rinsed with ethanol to obtain sensitized TiO₂ (denoted **2-TiO₂**).

The supplier of the N719 is EIC laboratories, Inc. The N719-TiO₂ NPs were prepared by stirring 15 mg of P25 in 60 mL of a 2 mM solution of N719 in ethanol at reflux for 12 h. The resulting nanoparticles were rinsed 3 times with ethanol, or until the ethanol remained colorless.

2. UV-visible Spectroscopic Measurements.

The samples for UV-visible spectroscopic measurements consist of thin mesoporous films (~10 μm thick) of Degussa P25 nanoparticles. The nanoparticles were doctor-bladed from aqueous solution onto a glass cover slip and annealed at 450 °C for 2 hours. The resulting slides were sensitized with **2** by stirring in dry ethanol at room temperature.² Films of P25 nanoparticles were highly scattering and spectra were obtained using a Varian Cary 3 spectrophotometer in diffuse reflectance geometry with an integrating sphere.

III. EPR Spectroscopy.

TiO₂ nanoparticles sensitized with [Mn^{II}(H₂O)₅(**2**)]²⁺ were prepared by stirring **2-TiO₂** with deionized H₂O and then soaking in a 2 mM aqueous solution of Mn(II) acetate for 2 hours. The resulting nanoparticles were washed with deionized H₂O, collected by centrifugation, and dried in the dark for EPR measurements. Perpendicular-mode EPR data were collected on an X-band Bruker Biospin/ELEXSYS E500 spectrometer equipped with a SHQ cavity and an Oxford ESR-900 liquid helium cryostat. All spectra were collected at 6 K on dry, powdered samples sealed in capillary tubes placed in 5 mm OD quartz EPR tubes containing 60/40 toluene/acetone which forms a transparent glass for efficient illumination of the sample and allows efficient heat transfer to prevent heating of the sample during illumination. Time-course measurements follow the signal intensity at 3106 G. All illuminations were carried out in the cryostat with white light passed through 420 nm long-pass and water filters. Relative Mn(II) concentrations are based on comparison of peak-to-peak amplitudes of both initial and illuminated signals at 3120 and 3667 G.

IV. Surface Coverage Determination

All samples were completely combusted in a Costech ECS 4010 elemental analyzer, and all N and C in the combustion products were quantified using a ThermoFinnigan DeltaPLUS Advantage mass spectrometer. The weight % of N is reported in Table S1. In addition, given that **2** has four N atoms and N719 has six, the wt. % can be converted to the number of moles of adsorbate per g of functionalized

* Corresponding Authors: robert.crabtree@yale.edu; gary.brudvig@yale.edu; victor.batista@yale.edu; charles.schmuttenmaer@yale.edu

TiO₂ NPs, which is then converted to a coverage in terms of molecules/nm² since it is well established that Degussa P25 has a specific surface area of 50 m²/g.^{3a} Thus, we find that the coverage of **2** is 1.20 molecules/nm², while that for N719 is 0.99 molecules/nm². Nazeeruddin et al.^{3b} report a coverage of 1.3×10^{-7} mol/“projected cm²” along with a roughness factor of ca. 1000 cm²/“projected cm²”, allowing one to calculate a surface coverage of 1.3 μM/m², or 0.81 molecules/nm².

Table S1. % Nitrogen by weight for **2-TiO₂** and N719-TiO₂ NPs. Values in parentheses are the 1 standard deviation uncertainties.

	2-TiO ₂	N719-TiO ₂
N (wt. %)	0.53844 ($1.3 \cdot 10^{-5}$)	0.66631 ($4.6 \cdot 10^{-3}$)
μM/g	96.107 ($2.3 \cdot 10^{-3}$)	79.285 ($5.4 \cdot 10^{-1}$)
molecules/nm ²	1.196 ($3 \cdot 10^{-5}$)	0.987 ($7 \cdot 10^{-3}$)

V. Time-Resolved Terahertz Spectroscopy Measurements.

An amplified Ti:sapphire laser (Tsunami/Spitfire from Spectra Physics) generating 800 mW of pulsed near-IR light at a 1 kHz repetition rate was used. The pulse width is ~100 fs and the center wavelength is 800 nm. Roughly 2/3 of the power is frequency doubled and then filtered to produce 50 mW of 400 nm light for the pump beam. The remainder of the near-IR light is used to generate and detect THz radiation using a 4-paraboloid arrangement that focuses the THz beam to a spot size of ~3 mm at the sample. Terahertz radiation is generated using optical rectification in a ZnTe(110) crystal and detected using free space electro-optic sampling in a second ZnTe(110) crystal. Terahertz data were taken at room temperature. The average of three samples was taken for each data set. Further information on the spectrometer and techniques has been reported in the literature.^{4,5}

Terahertz radiation is adsorbed by mobile electrons in the TiO₂ conduction band and is insensitive to electrons within the absorbed sensitizer. A decrease in broadband THz (0.2 – 2 THz) transmission in photoexcited samples compared to non-photoexcited samples indicates a higher electron density in the TiO₂. Injection time is measured by monitoring the change in THz transmission as the delay time between the 400 nm pump and the THz probe is varied.

Given that the refractive index of the films is 2.47,⁶ their thicknesses are determined by measuring the change in the arrival of THz waveforms transmitted through bare glass slides and transmitted through the same glass slide coated with the films. In each case, the additional delay due to the film was 55.4 ± 0.5 fs. Therefore, the film

$$\text{thickness is } \frac{55.4 \text{ fs} \times 0.3 \mu\text{m/fs}}{(2.47 - 1)} = 11.3 \mu\text{m}$$

VI. Computational Procedures.

To describe the attachment of **2** with TiO₂ nanoparticles, we used Density Functional Theory (DFT) calculations of the TiO₂ anatase (101) surface with the hydroxamate linker of **2** chelating a four-coordinate Ti⁴⁺ ion at an oxygen vacancy in the surface. The surface was represented by a slab, consisting of four layers of Ti⁴⁺ ions and eight layers of O²⁻ ions, that was periodically replicated in 3 dimensions. The dimensions of the slab were 10.49 Å × 15.18 Å × 5.9 Å in the [-101], [010] and [101] directions. A vacuum spacer of 10 Å was included to separate periodic slabs in the [101] direction.

The DFT calculations were performed using the plane-wave based Vienna Ab-initio Simulation Package (VASP).⁷⁻⁹ Vanderbilt Ultrasoft pseudopotentials were used to describe the core electrons.¹⁰ A 300 eV energy cutoff was used to truncate the plane-wave basis. Electron exchange and correlation were described using the PW91 generalized gradient approximation (GGA) functional. A $1 \times 1 \times 1$ Monkhorst-Pack k-point sampling was used to integrate over the

Brillouin zone. The geometry of the adsorbate and the six topmost layers of the TiO₂ slab were relaxed to the minimum energy configuration.

The binding enthalpies of hydroxamate anchors were estimated using benzohydroxamic acid as a model compound. The binding enthalpies were calculated by subtracting the energy of the clean surface and adsorbate in vacuum from the energy of the total system, adsorbate bound to the surface. The calculations predict that hydroxamate anchors bind 5 kcal/mol more strongly to the anatase (101) surface than benzoic acid, with an additional 5 kcal/mol of stabilization gained by dissociation of the nitrogen proton to a surface O²⁻ ion.

Simulations of IET were performed using the relaxed **2-TiO₂** slab extended 3×3 in the [-101] and [010] directions. The electronic structure of the complete model system was obtained using the extended Hückel method. The initial state of the electron was prepared by projecting the LUMO of **2** into the molecular orbitals of the complete model system. The goal of our simulation was not to model electron relaxation after a π-π* excitation of **2**, which occurs in the UV, but after a MLCT to the LUMO of **2** from a metal center immobilized in the terpyridine.

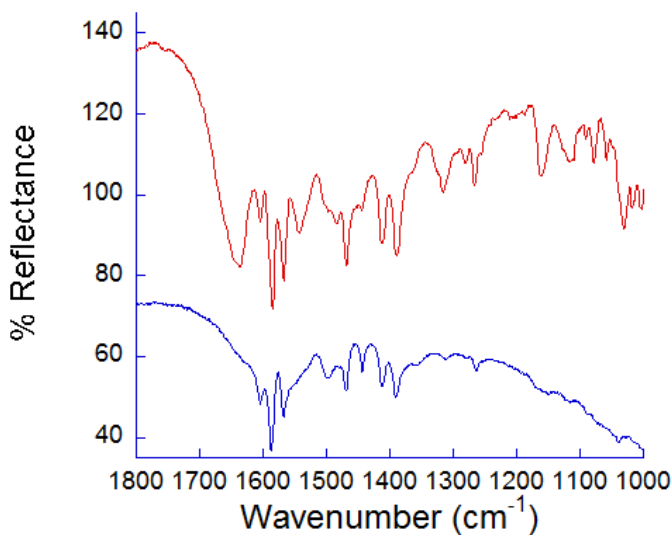


Figure S1. Diffuse Reflectance IR spectra of unbound **2** (red) and **2-TiO₂** (blue).

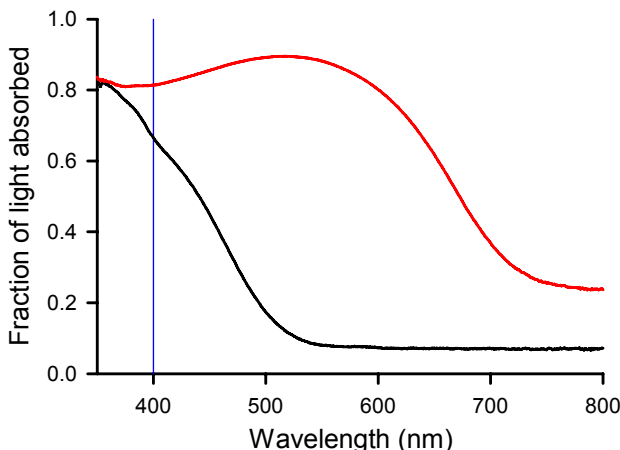


Figure S2. UV-visible spectra of **2**-TiO₂ (black) and N719-TiO₂ (red). The thin blue line represents the excitation wavelength of 400 nm.

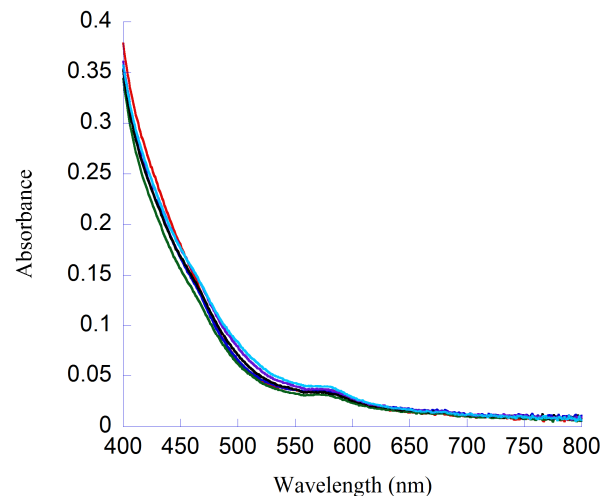


Figure S3. UV-visible spectra of **2**-TiO₂ after incubation in water for 0 hours (red), 1 hour (blue), 3 hours (green), 6 hours (black), 12 hours (purple), and 24 hours (light blue).

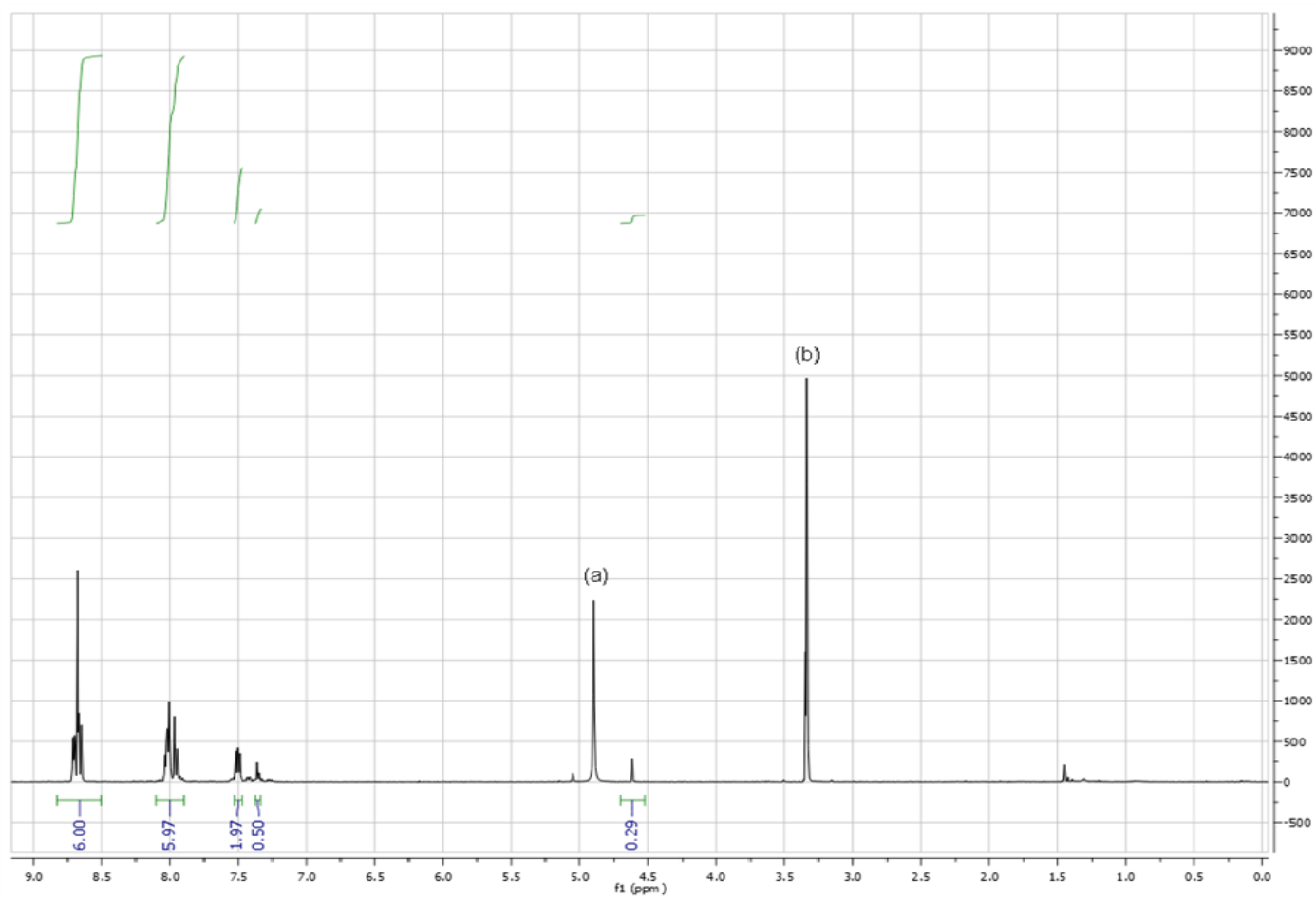


Figure S4. ^1H NMR spectrum of **2** in CD_3OD . Solvent residual peaks are noted at δ 4.87 (a), and 3.34 ppm (b) for water and methanol in CD_3OD , respectively.

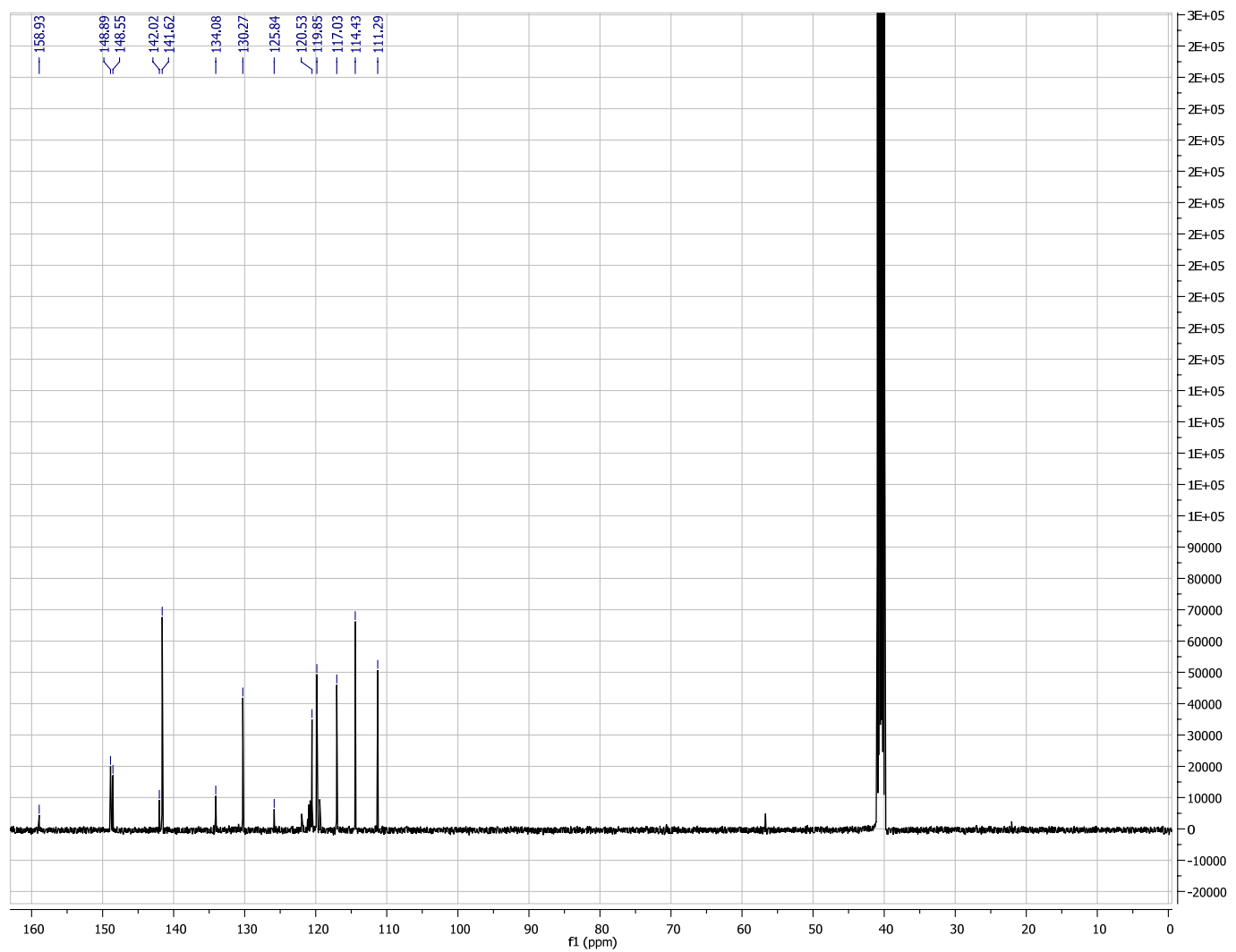


Figure S5. ^{13}C NMR spectrum of **2** in $(\text{CD}_3)_2\text{SO}$. A solvent residual peak is at δ 40.45 ppm for $(\text{CD}_3)_2\text{SO}$.

References

- (1) Wolpher, H.; Sinha, S.; Pan, J. X.; Johansson, A.; Lundqvist, M. J.; Persson, P.; Lomoth, R.; Bergquist, J.; Sun, L. C.; Sundstrom, V.; Akermark, B.; Polivka, T., "Synthesis and electron transfer studies of ruthenium-terpyridine-based dyads attached to nanostructured TiO₂," *Inorg. Chem.* **2007**, *46*, 638-651.
- (2) McNamara, W. R.; Snoeberger, R. C.; Li, G.; Schleicher, J. M.; Cady, C. W.; Poyatos, M.; Schmuttenmaer, C. A.; Crabtree, R. H.; Brudvig, G. W.; Batista, V. S., "Acetylacetone Anchors for Robust Functionalization of TiO₂ Nanoparticles with Mn(II)-Terpyridine Complexes," *J. Am. Chem. Soc.* **2008**, *130*, 14329-14338.
- (3)(a) Li, G.; Sproviero, E. M.; Snoeberger, R. C.; Iguchi, N.; Blakemore, J. D.; Crabtree, R. H.; Brudvig, G. W.; Batista, V. S. *Energy Environ. Sci.* **2009**, *2*, 230.
(b) Nazeeruddin, M. K.; Kay, A.; Rodicio, I.; Humphrybaker, R.; Muller, E.; Liska, P.; Vlachopoulos, N.; Grätzel, M., "Conversion of light to electricity by cis-X₂bis(2,2'-bipyridyl-4,4'-dicarboxylate)ruthenium(II) charge-transfer sensitizers (X = Cl⁻, Br⁻, I⁻, CN⁻, and SCN⁻) on nanocrystalline TiO₂ electrodes," *J. Am. Chem. Soc.* **1993**, *115*, 6382-6390.
- (4) Baxter, J. B.; Schmuttenmaer, C. A., "Conductivity of ZnO nanowires, nanoparticles, and thin films using time-resolved terahertz spectroscopy," *J. Phys. Chem. B* **2006**, *110*, 25229-25239.
- (5) Beard, M. C.; Turner, G. M.; Schmuttenmaer, C. A., "Transient photoconductivity in GaAs as measured by time-resolved terahertz spectroscopy," *Phys. Rev. B* **2000**, *62*, 15764-15777.
- (6) Turner, G. M.; Beard, M. C.; Schmuttenmaer, C. A., "Carrier localization and cooling in dye-sensitized nanocrystalline titanium dioxide," *J. Phys. Chem. B* **2002**, *106*, 11716-11719.
- (7) G. Kresse, G.; Hafner, J. *Phys. Rev. B* **1993**, *47*, 558; ibid. 1994, *49*, 14251.
- (8) Kresse, G.; Furthmuller, J. *Comput. Mat. Sci.* **1996** *6*, 15.
- (9) Kresse, G.; Furthmuller, J. *Phys. Rev. B* **1996**, *54*, 11169.
- (10) Kresse, G.; Hafner, J. *J. Phys.: Condens. Matt.* **1994**, *6*, 8245.